

Deep-learning-based precoding in multiuser MIMO downlink channels with limited feedback

Kyeongbo Kong, Woo-Jin Song *Member, IEEE*, and Moonsik Min *Member, IEEE*

Abstract—We propose a deep-learning-based channel quantization, feedback, and precoding method for downlink multiuser multiple-input multiple-output systems. In the proposed system, the traditional codebook-based channel quantization process for limited feedback is handled by a receiver deep neural network (DNN) for each user. The precoder selection process is handled by a transmitter DNN for the base station. At each receiver DNN, a binarization layer is adopted to emulate the channel quantization process and enable end-to-end learning. However, during training, receiver DNNs with the binarization layer can be trapped at a poor local minimum because of inaccurate gradients caused by the binarization layer. To address this, we consider a method of knowledge distillation, in which the existing DNNs are jointly trained with an additional auxiliary transmitter DNN. By using the auxiliary DNN as a teacher network, the receiver DNNs can additionally exploit lossless gradients, which is useful in avoiding a poor local minimum. Moreover, through joint training, the existing DNNs can be generalized including the quantization loss from binarization. All DNNs at the associated users and transmitter are trained offline in an end-to-end manner, with the aid of the auxiliary transmitter DNN. The purpose of the end-to-end learning is to determine the precoding matrices that maximize the downlink sum rate. Our DNN-based precoding scheme can achieve a significantly higher downlink rate compared to traditional linear precoding with codebook-based limited feedback, for the same number of feedback bits, particularly when the number of receive antennas is greater than one.

Index Terms—Deep learning, multiple-input multiple-output, limited feedback, spatial multiplexing, linear precoding.

I. INTRODUCTION

Multiuser multiple-input multiple-output (MU-MIMO) systems have been continuously studied to serve multiple users with high spectral efficiency. In downlink MU-MIMO systems, the transmitter at the base station (BS) is required to perform pre-signal processing before data transmission because joint signal processing is not possible among multiple users [1]–[4]; this process is generally called precoding. The transmitter requires channel state information (CSI) for appropriate precoding, and the downlink rate is significantly affected by the accuracy of the CSI at the transmitter (CSIT) [5], [6].

However, the transmitter cannot directly track the downlink channel in frequency division duplex (FDD) systems. Thus, channel quantization and feedback methods, called limited feedback, have been widely studied to achieve at least partial CSIT [5]–[12]. In limited feedback, each user estimates and

quantizes CSI, and then feeds the quantized index back to the transmitter. In practical systems, each feedback bit must be conveyed by using uplink communication resources, and the number of bits allocated for CSI feedback is not very large. Thus, the type of CSI for feedback should be carefully determined considering the purpose of the feedback. The channel direction information (CDI) of the channel matrix, which is given by a unitary matrix, is commonly considered for supporting the precoding design because CDI can directly be used to reduce multiuser interference in the received signals [5], [6], [11]. CDI can be used to perform useful zero-forcing linear precoding, which is known to achieve a considerably high downlink rate, assuming perfect CSIT [13]–[16]. However, with limited feedback, the performance is limited if the number of feedback bits is insufficient [5], [6]. Consequently, the application of MU-MIMO is limited in practical FDD-based downlink systems (it is often recommended in a low signal-to-noise ratio (SNR) regime, e.g., the case of cell edge users). Thus, the achievable downlink rate of limited-feedback-based MU-MIMO systems needs to be increased; however, this is a challenging task.

Recently, deep-learning-based methods have been studied to improve the performance of limited feedback for MIMO systems. In [17], to improve the accuracy of the CSIT, a CSI sensing and recovery network was designed using a convolutional neural network. The authors in [18] further used a recurrent neural network (RNN) that captures the time correlation to enhance the channel recovery module. Recurrent compression and uncompression modules for RNN design were further studied in [19]. In [20], a deep auto-encoder was constructed to reduce the impact of the feedback errors and delay during CSI feedback. Thus far, studies have focused on improving the accuracy of CSIT. The authors in [21] proposed a deep neural network (DNN)-based beamforming method with limited feedback for a single-user single-stream downlink MIMO system. Two individual DNNs were implemented at the user and the BS. These DNNs were trained in an end-to-end manner by introducing a binarization layer, which was used to effectively model the quantization process of the CSI. The trained DNNs efficiently abstract the joint process of channel estimation, quantization, and beamformer selection. Thus, this method can achieve a gain of approximately 1 dB in terms of symbol-error-rate performance.

The novel structure proposed in [21] applied a binarization layer that could effectively abstract the quantization process of the conventional limited feedback system without constructing an explicit codebook. The receiver DNN replaced the role of the conventional codebook-based channel quantization

process. However, the performance achieved by realizing the quantization and beamformer selection with DNNs is similar to that of the conventional codebook-based approach. The gain mainly originates from the joint optimization of the channel estimation and quantization process based on the use of the DNN. This is because individual problems of channel quantization and the beamforming selection for a single-stream transmission over multiple transmit and receive antennas already have near-optimal mathematical (or analytical) solutions.

However, suppose that we consider multi-stream spatial multiplexing in general MU-MIMO downlink channels, in which a single BS simultaneously communicates with multiple users who have multiple receive antennas and all the receive antennas can be used for spatial multiplexing. Then, the problems of determining an optimal quantization codebook, optimal distance measure, and optimal precoder are extremely challenging. Thus, if a data-driven solution based on deep learning can achieve the joint optimization of the codebook design, distance measure design, and precoder selection, the performance may be significantly better than that of the conventional MU-MIMO systems using codebook-based limited feedback. This is the primary objective of this study.

In this study, we extend the work in [21] to full-stream MU-MIMO downlink systems with limited feedback, in which each user can have multiple receive antennas. We focus on the scenarios in which the transmitter allocates equal power to the associated users (i.e., we do not consider a specific power allocation) to consider a fair transmission rate for the associated users. This is a common assumption in conventional MU-MIMO systems with limited CDI feedback [5], [6], as a sophisticated power allocation is not possible with only partial CDI at the transmitter. Thus, for a direct comparison with the baseline limited-feedback-based systems, we assume equal power allocation among the associated users in this study.¹ In the proposed system, individual DNNs are implemented for the users and the BS. To enable end-to-end learning, a binarization layer is adopted at each receiver DNN as was done in [21]. However, the binarization operation in the corresponding layer can cause a vanishing gradient problem in backpropagation during the end-to-end learning. To address this, we employ pseudo-gradients using straight-through estimator (STE) [22]. The pseudo-gradients may not be in the right direction for updating the parameters; thus, DNNs can be trapped at a poor local minimum [23], [24]. Accordingly, a joint training method is proposed in this study, in which the existing DNNs are efficiently trained with the aid of an auxiliary teacher network. Because each receiver DNN in the proposed system has only one lossy layer with binarization, we can directly provide lossless gradients to the receiver DNNs by simply adding an

auxiliary transmitter DNN, which has the same structure as the existing transmitter DNN. Then, end-to-end learning is jointly performed to determine the precoding matrices that maximize the downlink sum rate, which is given by the sum of the log-determinants of a function of channel and precoding matrices. The proposed data-driven solution for the precoding matrices outperforms the simple and widely used zero-forcing linear precoding (possibly regularized) method, particularly when the number of receive antennas is greater than one. Moreover, an optimal codebook design or an optimal distance measure need not be considered, as the trained receiver DNN of each user can jointly optimize the corresponding processes based on data-driven training.

Our loss function of the end-to-end learning is the sum rate, which depends on the transmit power of the system. Therefore, the transmitter DNN in this study also considers the transmit power as an input, and the corresponding structure can be used to further construct a unified transmit DNN applicable for different values of the transmit power. That is, as a practical application, the transmit power can be trained during the end-to-end learning process, and the resulting transmitter DNN can determine the appropriate precoding matrices for any value of the transmit power in a predefined range without additional training.

In a parallel study [25], the authors recently extended the work in [21] to massive MIMO and millimeter-wave channels, and they proposed the joint optimization of pilot selection, channel estimation, quantization, beamforming selection, and power allocation to increase the sum rate of the system when each user has a single receive antenna. The corresponding results are suitable for future wireless standards based on millimeter-wave transmission with massive transmit antennas. In contrast, we consider a more practical and traditional limited-feedback-based MU-MIMO scenario in which equal power allocation is used for a fairer data-rate allocation to the associated users, and the number of feedback bits for each user is relatively small. Simultaneously, we consider a more general antenna configuration, in which each user can have multiple receive antennas for spatial multiplexing. For baseline systems, regularized zero-forcing precoding methods are also considered, as they perform better than the normal zero-forcing precoding methods. Then, we focus on improving the deep learning performance of the proposed DNN-based MU-MIMO systems; a joint training method with an auxiliary (teacher) network is proposed to further improve the performance of deep learning. Based on the proposed joint training, we analyze the improvement realized solely by replacing the role of the conventional channel quantization and precoding selection process with the proposed DNNs, without considering the potential gain from the joint channel estimation and quantization. The proposed DNN-based limited feedback and precoding selection can achieve a significantly higher sum rate than the baseline systems, particularly when the number of receive antennas of each user is greater than one. Moreover, the gain increases with the number of receive antennas for a fixed number of total feedback bits.

Notations: The matrices and column vectors are denoted by upper- and lower-case boldface letters, respectively. The

¹In fact, the deep-learning-based solution proposed in this paper can also handle power allocation, as it does not send, in effect, explicit CSI by abstracting the quantization and feedback process with DNNs. This can also be an advantage over the conventional systems, as the latter systems additionally require information about channel gains to design a specific power allocation. However, if the number of feedback bits is not sufficient, our deep-learning-based solution with power allocation, which simply maximizes the sum rate, tends to allocate all the transmit power to a small portion of users. This is not desirable for systems considering a fair transmission rate to the associated users and this is another reason for assuming equal power allocation.

superscripts $(\cdot)^T$ and $(\cdot)^H$ indicate the transpose and complex conjugate transpose of a matrix, respectively. The operators $\text{tr}(\cdot)$ and $\det(\cdot)$ indicate the trace and determinant of a matrix, respectively. The sets \mathbb{R} and \mathbb{C} represent the sets of real and complex numbers, respectively, and $\mathbb{C}^{m \times n}$ denotes the set of all $m \times n$ complex matrices. \mathbf{I}_m is an $m \times m$ identity matrix. $\mathbb{E}(\cdot)$ indicates the expectation operator.

II. BASELINE SYSTEM MODEL

This study considers conventional precoding methods in MU-MIMO channels based on limited feedback as a baseline system. In particular, we consider a MIMO broadcast channel in which K users communicate with a single BS. The BS is equipped with M transmit antennas, and each user has N receive antennas. We assume that M is a multiple of N and $M > N$. The MIMO channels between the BS and users $k \in \{1, \dots, K\}$ are modeled as independent channel matrices $\mathbf{H}_k \in \mathbb{C}^{M \times N}$, $k = 1, \dots, K$, where the entries of each matrix are independent and identically distributed (i.i.d.) complex Gaussian random variables with zero mean and unit variance. The received signal of user k is given by

$$\mathbf{y}_k = \mathbf{H}_k^H \mathbf{x} + \mathbf{n}_k, \quad (1)$$

$k = 1, \dots, K$, where \mathbf{x} is the transmit vector and \mathbf{n}_k is a complex Gaussian noise vector with independently distributed entries of zero mean and unit variance. The transmit vector is given by $\mathbf{x} = \sum_{l=1}^K \mathbf{V}_l \mathbf{s}_l$, where $\mathbf{V}_l \in \mathbb{C}^{M \times N}$ is the precoding matrix; we assume $\text{tr}(\mathbf{V}_l^H \mathbf{V}_l) = N$ to realize equal power allocation to users. The information symbol vector $\mathbf{s}_l \in \mathbb{C}^{N \times 1}$ consists of N independent data symbols for the user l such that each user is fully served with N degrees of spatial multiplexing. In addition, we do not consider specific user selection, and we assume that $K \leq M/N$. We impose the power constraint P at the BS, and the transmit power allocation for data streams is $\mathbb{E}[\mathbf{s}_l \mathbf{s}_l^H] = \frac{P}{M} \mathbf{I}_N$ to achieve equal power allocation to users.

A. Limited feedback model

In MIMO broadcast channels, the BS can achieve at most M spatial multiplexing gain through simultaneous communication with multiple users. Accordingly, the transmitter should have CSIT to achieve this gain. In this study, we consider a widely studied limited feedback model to allow partial CSIT [5], [6]. In the corresponding model, each user quantizes and feeds back CDI to the transmitter, where the CDI is represented by a unitary matrix of singular value decomposition (SVD). We assume perfect channel estimation at the receiver because we do not consider a potential gain from the joint channel estimation and quantization; such a gain from joint optimization was sufficiently discussed in [21], and thus, it is evident. Instead, in this study, we focus on the advantage of replacing the role of the conventional quantization and precoding process with DNNs in limited-feedback-based MU-MIMO systems.

Let $\mathbf{H}_k = \tilde{\mathbf{H}}_k \Sigma_k^{\frac{1}{2}} \mathbf{U}_k^H$ represent the compact SVD of the channel matrix. As quantizing the entire matrix \mathbf{H}_k is inefficient (it requires a large number of feedback bits), a typical limited feedback model quantizes and feeds back the

unitary matrix $\tilde{\mathbf{H}}_k \in \mathbb{C}^{M \times N}$ containing the direction information of the channel. User k quantizes $\tilde{\mathbf{H}}_k$ using codebook $\mathcal{C}_k = \{\mathbf{A}_{k,1}, \dots, \mathbf{A}_{k,2^B}\}$, which is fixed beforehand for each user and is known to the transmitter. Each codeword $\mathbf{A}_{k,j}$ is given by a semi-unitary matrix in $\mathbb{C}^{M \times N}$ such that $\mathbf{A}_{k,j}^H \mathbf{A}_{k,j} = \mathbf{I}_N$, and it is different from all other codewords. Denoting $\mathcal{J} = \{1, \dots, 2^B\}$ as the index set for the codewords, the quantization process can be expressed as

$$q_k = \underset{j \in \mathcal{J}}{\text{argmin}} d(\mathbf{A}_{k,j}, \tilde{\mathbf{H}}_k), \quad (2)$$

where $d(\cdot, \cdot)$ is a distance measure. Each user feeds back index q_k to the transmitter, and the transmitter can obtain a quantized channel matrix $\hat{\mathbf{H}}_k = \mathbf{A}_{k,q_k}$ from codebook \mathcal{C}_k .

B. Performance metric

From (1), the per-user achievable rate of limited-feedback-based precoding is given by

$$R_k \triangleq \mathbb{E} \left[\log_2 \left| \mathbf{I}_N + \frac{P}{M} \sum_{l=1}^K \mathbf{H}_k^H \mathbf{V}_l \mathbf{V}_l^H \mathbf{H}_k \right| \right] - \mathbb{E} \left[\log_2 \left| \mathbf{I}_N + \frac{P}{M} \sum_{l=1, l \neq k}^K \mathbf{H}_k^H \mathbf{V}_l \mathbf{V}_l^H \mathbf{H}_k \right| \right]. \quad (3)$$

Let $G(\cdot)$ be a function that outputs precoding matrices $\mathbf{V}_1, \dots, \mathbf{V}_K$ by considering quantized channels $\hat{\mathbf{H}}_1, \dots, \hat{\mathbf{H}}_K$ as input, such as $\mathbf{V} = [\mathbf{V}_1 \dots \mathbf{V}_K] = G([q_1, \dots, q_K])$, with $\text{tr}(\mathbf{V}_l^H \mathbf{V}_l) = N$, $l = 1, \dots, K$. Then, in terms of capacity, an optimal precoder is a solution to the following optimization problem:

$$\max_{G(\cdot)} \sum_{k=1}^K R_k(G([q_1, \dots, q_K])), \quad (4)$$

$$\text{subject to } q_k = \underset{j \in \mathcal{J}}{\text{argmin}} d(\mathbf{A}_{k,j}, \mathbf{H}_k), \forall k = 1, \dots, K. \quad (5)$$

C. Precoding

Designing precoding at the transmitter is equivalent to determine a mapping function $G(\cdot)$ from quantized CSIs to the precoding matrices, as described in the previous subsection. With limited feedback, one of the most famous methods is zero-forcing-type linear precoding: zero-forcing beamforming (ZFBF) when $N = 1$ [5] and block diagonalization (BD) when $N > 1$ [6]. Zero-forcing precoding (possibly regularized) is useful in practice, as a high downlink sum rate with relatively low complexity can be achieved; further, zero-forcing precoding is feasible only with CDI feedback, which is typical in the case of limited feedback [11].

If the transmitter has perfect CSI, an iterative method, called weighted minimum mean squared error (WMMSE) precoding, provides a local optimal solution for the linear precoding design; furthermore, the performance achieved by WMMSE is near to the capacity achieved by using dirty paper coding [26]. Similarly, other iterative methods have been studied based on regularized BD (RBD) to achieve near-optimal performance [16]. However, to realize such a near-optimal linear precoding

based on iterations, the transmitter must have an accurate estimate of the entire channel matrix \mathbf{H} rather than the CDI $\hat{\mathbf{H}}_k$. That is, additional feedback is required to send the quantized information of Σ_k , and statistics of the quantization error are further required to mitigate the performance degradation caused by the quantization error [27]. Moreover, the sum rate enhancement largely relies on the dynamic power allocation among users in succeeding iterations. Thus, these iterative approaches are not suitable for our limited feedback model.²

In conclusion, we do not consider iterative methods such as WMMSE or iterative RBD in this study. We consider normal and regularized zero-forcing linear precoding schemes, which have a high efficiency among existing linear precoding schemes with limited feedback in terms of achievable rate per feedback bit, as baseline systems.

1) *ZFBF*: If $N = 1$, \mathbf{H}_k and \mathbf{V}_k are given by vectors and thus, the quantized CDI is also given by a vector. For simplicity, let $\hat{\mathbf{h}}_k$ be the quantized CDI of user k . ZFBF is based on channel inversion using precoding vectors. Defining

$$\tilde{\mathbf{H}}_{\text{ZF}} = [\hat{\mathbf{h}}_1, \dots, \hat{\mathbf{h}}_K], \quad (6)$$

$$\mathbf{F}_{\text{ZF}} = \tilde{\mathbf{H}}_{\text{ZF}} (\tilde{\mathbf{H}}_{\text{ZF}}^H \tilde{\mathbf{H}}_{\text{ZF}})^{-1}. \quad (7)$$

The ZFBF vector of user k is given by the k -th normalized column vector of \mathbf{F}_{ZF} . Regularization can enhance the performance of ZFBF, and the corresponding method is called regularized zero-forcing (RZF). In RZF, the beamforming vector of user k is given by the k -th normalized column vector of the following matrix:

$$\mathbf{F}_{\text{RZF}} = \tilde{\mathbf{H}}_{\text{ZF}} (\tilde{\mathbf{H}}_{\text{ZF}}^H \tilde{\mathbf{H}}_{\text{ZF}} + \alpha_{\text{ZF}} \cdot \mathbf{I})^{-1}. \quad (8)$$

If the transmitter has perfect CSI, the regularization parameter α_{ZF} is given by $\alpha_{\text{ZF}} = \frac{KN}{P}$ [15]. As we use limited feedback, α_{ZF} must be determined by reflecting the quantization error [28].

2) *BD*: BD is also based on channel inversion similar to ZFBF; however, the BD precoding matrix of user k does not need to invert its own channel \mathbf{H}_k , as joint signal processing is possible at the user among the N received signals of the user. The precoding matrix \mathbf{V}_k is selected to satisfy $\mathbf{H}_l^H \mathbf{V}_k = \mathbf{0}$ for $l \neq k$. However, with limited feedback, the transmitter only knows quantized channel matrices $\{\hat{\mathbf{H}}_l : l = 1, \dots, K\}$ that are fed back from the users. Thus, instead, the precoding matrix of limited-feedback-based BD is selected to satisfy $\hat{\mathbf{H}}_l^H \mathbf{V}_k = \mathbf{0}$ for $l \neq k$, such that the columns of \mathbf{V}_k lie in the null space of the following matrix [6]:

$$\Phi_k = [\hat{\mathbf{H}}_1 \dots \hat{\mathbf{H}}_{k-1} \hat{\mathbf{H}}_{k+1} \dots \hat{\mathbf{H}}_K]^H \in \mathbb{C}^{N(K-1) \times M}. \quad (9)$$

Let the SVD of Φ_k be $\Phi_k = \mathbf{E}_{k,0} \mathbf{D}_{k,0} (\mathbf{G}_{k,0})^H$ such that $\mathbf{D}_{k,0} \in \mathbb{C}^{N(K-1) \times M}$ and $\mathbf{G}_{k,0} \in \mathbb{C}^{M \times M}$. Further, let $\tilde{\mathbf{G}}_{k,0} \in \mathbb{C}^{M \times (M-N(K-1))}$ be the matrix whose i -th column is equal

to the $(N(K-1) + i)$ -th column of $\mathbf{G}_{k,0}$ for $1 \leq i \leq M - N(K-1)$, and let

$$\mathbf{F}_k^{\text{BD}} = \hat{\mathbf{H}}_k^H \tilde{\mathbf{G}}_{k,0} \in \mathbb{C}^{N \times (M-N(K-1))}. \quad (10)$$

Denoting the compact SVD of \mathbf{F}_k^{BD} as $\mathbf{F}_k^{\text{BD}} = \mathbf{E}_{k,1} \mathbf{D}_{k,1} (\mathbf{G}_{k,1})^H$ (such that $\mathbf{D}_{k,1} \in \mathbb{C}^{N \times N}$ and $\mathbf{G}_{k,1} \in \mathbb{C}^{(M-N(K-1)) \times N}$), the BD precoding matrix for user k is given by $\mathbf{V}_k = \tilde{\mathbf{G}}_{k,0} \mathbf{G}_{k,1}$.

In RBD, the precoding matrix of user k does not always lie in the null space of Φ_k , to maintain a trade-off between mitigating the effects of noise and multiuser interference [16]. Let

$$\mathbf{F}_{k,0}^{\text{RBD}} = \hat{\mathbf{H}}_k^H \mathbf{G}_{k,0} (\mathbf{D}_{k,0}^H \mathbf{D}_{k,0} + \alpha_{\text{BD}} \cdot \mathbf{I})^{-\frac{1}{2}} \in \mathbb{C}^{N \times M}, \quad (11)$$

where α_{BD} is the regularization parameter for the BD. Denoting the compact SVD of $\mathbf{F}_{k,0}^{\text{RBD}}$ as $\mathbf{F}_{k,0}^{\text{RBD}} = \mathbf{E}_{k,2} \mathbf{D}_{k,2} (\mathbf{G}_{k,2})^H$ (such that $\mathbf{D}_{k,2} \in \mathbb{C}^{N \times N}$ and $\mathbf{G}_{k,2} \in \mathbb{C}^{M \times N}$), we define

$$\mathbf{F}_{k,1}^{\text{RBD}} \triangleq \mathbf{G}_{k,0} (\mathbf{D}_{k,0}^H \mathbf{D}_{k,0} + \alpha_{\text{BD}} \cdot \mathbf{I})^{-\frac{1}{2}} \mathbf{G}_{k,2}. \quad (12)$$

Then, as we consider equal power allocation to users, the RBD precoding matrix for user k is given by

$$\mathbf{V}_k = \sqrt{\frac{N}{\text{tr}(\mathbf{F}_{k,1}^{\text{RBD}})}} \cdot \mathbf{F}_{k,1}^{\text{RBD}}. \quad (13)$$

If the transmitter has perfect CSI, the regularization parameter α_{BD} is given by $\alpha_{\text{BD}} = \frac{KN}{P}$ [16]. With limited feedback, the optimal value of α_{BD} depends on the quantization error, similar to the case of RZF.

As both BD and RBD cannot eliminate multiuser interference with limited feedback, the received signal of user k can be rewritten as

$$\mathbf{y}_k = \mathbf{H}_k^H \mathbf{V}_k \mathbf{s}_k + \sum_{l=1, l \neq k}^K \mathbf{H}_k^H \mathbf{V}_l \mathbf{s}_l + \mathbf{n}_k. \quad (14)$$

In (14), the summation term corresponds to the multiuser interference caused by the quantization error.

The fundamental logic behind zero-forcing precoding is to eliminate multiuser interference. This method achieves high performance with perfect CSIT because the transmitter can mathematically obtain the precoding matrices that perfectly eliminate multiuser interference in the received signals. However, with limited feedback, an avoidable quantization error exists for the CSI available at the transmitter, which causes significant multiuser interference when the number of feedback bits is not sufficiently large. Consequently, BD cannot effectively suppress multiuser interference, although the use of BD is intended to eliminate it. The regularization parameter can be used to mitigate such a problem; however, it is still not sufficient and obtaining an optimal regularization parameter considering the quantization error is difficult. Thus, this study considers a deep-learning-based solution as an alternative solution to generate precoding matrices that perform better than the zero-forcing precoding schemes described in this section.

²In fact, it is not feasible to implement them with only the CDI feedback. Although we succeeded in implementing them with some additional CSI feedback, they cannot achieve the expected performance unless the number of feedback bits is very large.

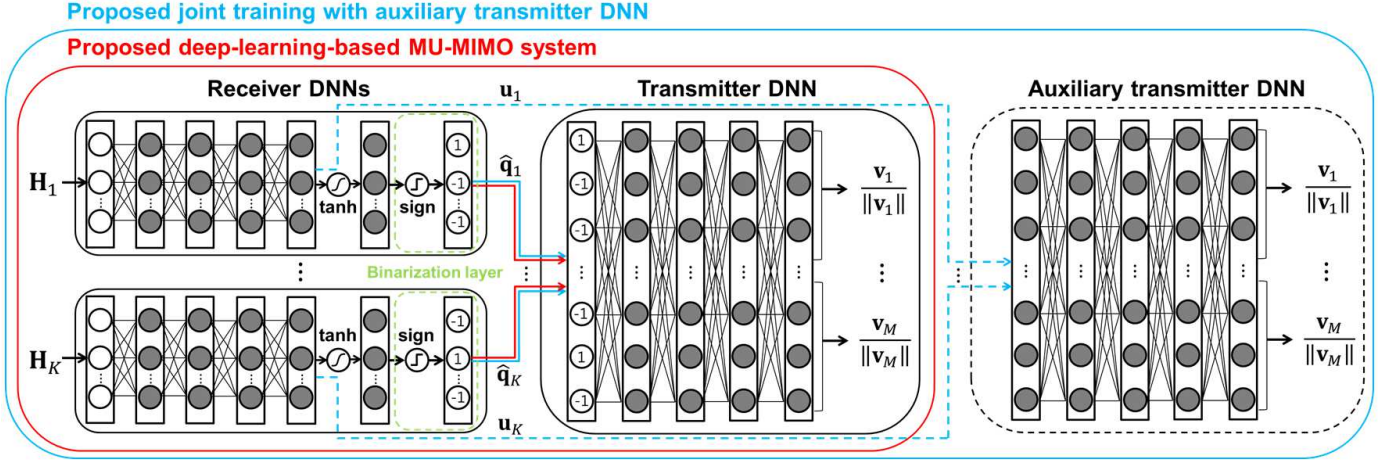


Fig. 1. Schematic of the proposed deep-learning-based MU-MIMO system with joint training method. In the proposed deep-learning-based MU-MIMO system, receiver DNNs estimate feedback information for each input channel, and these estimated informations are used as input to the transmitter DNN (red solid line). The transmitter DNN estimates precoding matrices, where the columns of each precoding matrix are normalized. In the training phase, receiver DNNs are connected with both transmitter DNN (blue solid line) and auxiliary transmitter DNN (blue dotted line). Then, joint training is performed to use a lossless gradient from auxiliary DNN to the receiver DNNs as well as the lossy gradient (due to binarization layer) from the transmitter DNN to the receiver DNNs.

III. PROPOSED DNN-BASED SYSTEM

A. Basic operation of a fully connected DNN

Denoting D_n as the dimension of the n -th hidden layer of a fully connected network, the output \mathbf{z}_n of the n -th hidden layer is given by [21]

$$\mathbf{z}_n = a(\mathbf{W}_n \mathbf{z}_{n-1} + \mathbf{b}_n), \quad (15)$$

where $a(\cdot)$ is an element-wise activation function, $\mathbf{W}_n \in \mathbb{R}^{D_n \times D_{n-1}}$ is a weight matrix, and $\mathbf{b}_n \in \mathbb{R}^{D_n \times 1}$ is a bias vector. In this study, we exploit a rectified linear unit (ReLU) activation [29] denoted by $a(x) = \max(0, x)$. Denoting t as the number of total hidden layers in a fully connected network, the output of DNN \mathbf{z}_t is obtained by recursively applying (15); note that the activation function is not applied at the last recursion. Let Θ be the set of all parameters of the corresponding fully connected network. Then, the output can be expressed as

$$\mathbf{z}_t = \text{FC}(\mathbf{z}_0; \Theta). \quad (16)$$

A general fully connected network described in (16) is implemented for each user and the BS.

B. Proposed deep-learning-based MU-MIMO system

In this paper, an end-to-end deep-learning-based system is proposed in which the BS and users have individual fully connected networks (Fig. 1; red box). The receiver DNN abstracts the channel quantization process; it outputs a quantization index, which will be fed back to the BS, by considering its individual channel as an input. Denoting the input-output relation of the receiver DNN of user k as a mapping function $f_k^R(\cdot)$, the quantization process can be modeled as

$$\hat{\mathbf{q}}_k = f_k^R(\mathbf{H}_k; \Theta_k^R), \quad (17)$$

where Θ_k^R is the parameter set of a fully-connected network included in the receiver DNN of user k and $\hat{\mathbf{q}}_k$ is a vector of

size B and each element of $\hat{\mathbf{q}}$ is 1 or -1 ; thus, it has a one-to-one correspondence with the feedback index q_k of the baseline limited feedback system. The transmitter DNN determines the precoding matrices \mathbf{V}_k , $k = 1, \dots, K$ by combining the feedback information from users. The corresponding input-output relation is denoted by a mapping function f^T as follows:

$$\mathbf{V} = [\mathbf{V}_1 \cdots \mathbf{V}_K] = f^T(\hat{\mathbf{q}}_1, \dots, \hat{\mathbf{q}}_K, P; \Theta^T), \quad (18)$$

where Θ^T is the parameter set of a fully-connected network included in the transmitter DNN. Consequently, the optimization problem in (4)-(5) is modified to

$$\max_{\Theta^T, \Theta_1^R, \dots, \Theta_K^R} \sum_{k=1}^K R_k(f^T(\hat{\mathbf{q}}_1, \dots, \hat{\mathbf{q}}_K, P; \Theta^T)), \quad (19)$$

$$\text{subject to } \hat{\mathbf{q}}_k = f_k^R(\mathbf{H}_k; \Theta_k^R), \forall k = 1, \dots, K. \quad (20)$$

C. Details of receiver DNNs and transmitter DNN

At each user k , channel \mathbf{H}_k is first converted to a real vector, and then used as an input to the receiver DNN implemented at the user. Let \mathbf{h}_k^C be a complex vector obtained by stacking the columns of \mathbf{H}_k one after another from first to the last column. Then, $\mathbf{h}_k^{\text{Re}} = [\text{Re}(\mathbf{h}_k^C)^T \text{Im}(\mathbf{h}_k^C)^T]^T$ is an input to the receiver DNN at user k . Based on the operation described in Section III-A, a fully connected network FC_k^R at user k is used to estimate a real-valued output vector $\mathbf{u}_k \in \mathbb{R}^{B \times 1}$ as $\mathbf{u}_k = \text{FC}_k^R(\mathbf{h}_k^{\text{Re}}; \Theta_k^R)$. Then, each element of this vector is binarized using the sign function after passing through the hyperbolic tangent function to obtain feedback information (Fig. 1; green box). Denoting the i -th element of \mathbf{u}_k as $[\mathbf{u}_k]_i$, the input-output relation of the receiver DNN $f_k^R(\cdot)$ in (17) is given by

$$\begin{aligned} \hat{\mathbf{q}}_k &= f_k^R(\mathbf{H}_k, \Theta_k^R) \\ &= [\text{sign}(\tanh([\mathbf{u}_k]_1)), \dots, \text{sign}(\tanh([\mathbf{u}_k]_B))]. \end{aligned} \quad (21)$$

The input-output relation of the transmitter DNN f^T in (18) is defined by using a fully connected network FC^T from $(\mathbf{x}_1, \dots, \mathbf{x}_K, x) \in \mathbb{R}^{B \times 1} \times \dots \times \mathbb{R}^{B \times 1} \times \mathbb{R}$ to $\mathbf{y} \in \mathbb{R}^{2MNK \times 1}$ with the parameter set Θ^T for training:

$$\mathbf{y} = \text{FC}^T(\mathbf{x}_1, \dots, \mathbf{x}_K, x; \Theta^T), \quad (22)$$

and a function h from $\mathbf{y} \in \mathbb{R}^{2MNK \times 1}$ to $\mathbf{Z} \in \mathbb{C}^{M \times NK}$:

$$\mathbf{Z} = h(\mathbf{y}). \quad (23)$$

For each $\mathbf{y} \in \mathbb{R}^{2MNK \times 1}$, the function h first maps \mathbf{y} to the complex vector $\mathbf{y}^C \in \mathbb{C}^{MNK \times 1}$, which is constructed as $\mathbf{y}^C = \mathbf{y}^{\text{Re}} + i\mathbf{y}^{\text{Im}}$, where \mathbf{y}^{Re} and \mathbf{y}^{Im} correspond to the first and second halves of \mathbf{y} , respectively. Then, \mathbf{y}^C is mapped to $\bar{\mathbf{Z}} \in \mathbb{C}^{M \times NK}$, where the (i, j) -th element of $\bar{\mathbf{Z}}$ is equal to the $(M(j-1) + i)$ -th element of \mathbf{y}^C . Then, the output matrix \mathbf{Z} of the function h is obtained by normalizing every column of $\bar{\mathbf{Z}}$.

Using (22) and (23), the input-output relation of the transmitter DNN f^T in (18) is given by

$$\begin{aligned} \mathbf{V} &= f^T(\hat{\mathbf{q}}_1, \dots, \hat{\mathbf{q}}_K, P; \Theta^T) \\ &= h(\text{FC}^T(\hat{\mathbf{q}}_1, \dots, \hat{\mathbf{q}}_K, P; \Theta^T)). \end{aligned} \quad (24)$$

The binarized outputs of the receiver DNNs are connected to the transmitter DNN (Fig. 1) such that constraint (20) can be removed during end-to-end learning. That is, our overall training problem can be expressed as

$$\min_{\Theta^T, \Theta_1^R, \dots, \Theta_K^R} L_{\text{main}}(\{\Theta_k^R\}_{k=1}^K, \Theta^T), \quad (25)$$

where

$$\begin{aligned} L_{\text{main}}(\{\Theta_k^R\}_{k=1}^K, \Theta^T) \\ = - \sum_{k=1}^K R_k(f^T(\{f_k^R(\mathbf{H}_k; \Theta_k^R)\}_{k=1}^K, P; \Theta^T)). \end{aligned} \quad (26)$$

D. Joint training method for knowledge distillation

To map the real-valued output vector \mathbf{u}_k of each receiver DNN to a binary sequence of 1 or -1, we may directly apply one of the common binarization operators (e.g., $\text{sign}(\cdot)$, etc.). However, when these non-differentiable operators are used in the end-to-end learning process, the vanishing gradient problem can occur during backpropagation. To overcome this problem, most studies have employed the STE [22], which replaces the binarization operator with a smooth differentiable function in the backward pass. That is, a smooth differentiable function layer is added in front of the binarization layer, and the binarization layer is only exploited in the forward pass. In this study, we exploit the hyperbolic tangent function as a smooth differentiable function, similar to the study [21] (Fig. 1). Then, for the binarization layer, we exploit the approximated gradient of $\text{sign}(\tanh(z))$ in the backward pass as follows:

$$\nabla_{\Theta_k^R} \text{sign}(\tanh(z)) \approx \nabla_{\Theta_k^R} \tanh(z). \quad (27)$$

By using the STE, we can train the receiver DNNs and transmitter DNN in an end-to-end manner. However, according

to [23], [24], [30], the approximated gradient of the binarization function causes a noisy signal when updating the DNN parameters because the updating direction may be incorrect. Therefore, the receiver DNNs can be trapped at a poor local minima, and consequently, the performance may be degraded. Moreover, this error can be propagated to the transmitter DNN because of end-to-end learning.

To mitigate this, we consider knowledge distillation [31]–[35], where a deep teacher network distills knowledge to a shallow student network for training the student network well with respect to generalization. The key issue in knowledge distillation is to effectively transfer knowledge from a deep teacher network to a shallow student network. However, most layers of the shallow student network are bottlenecks in the training phase compared with those of the deep teacher network (i.e., because most layers of the shallow student network have generally different structures from those of the deep teacher network). Therefore, it is difficult to transfer knowledge to the corresponding layers effectively. In [31], the knowledge of deep teacher network was transferred by indirectly using softmax output, and [33] utilized additional hidden layers to map the hidden layers of student network to the hidden layers of teacher network. However, these methods have information loss caused by a mismatch between the structures of the teacher and student networks.

Unlike these problems, our study has only a single bottleneck at the end of the receiver DNN. In other words, the shallow student network and deep teacher network have identical structures, except for the binarization layer. Therefore, if we connect an auxiliary transmitter DNN to the outputs of the layer right before the hyperbolic tangent layer of the receiver DNNs (blue dotted line in Fig. 1), we can directly provide a lossless gradient to the receiver DNNs during end-to-end learning (Fig. 1; blue box). The input-output relation of the auxiliary transmitter DNN, which has the same network structure but different training parameters and input range compared with the existing transmitter DNN, is defined as follows:

$$\begin{aligned} \mathbf{V} &= f^T(\mathbf{u}_1, \dots, \mathbf{u}_K, P; \Theta_{\text{aux}}^T) \\ &= h(\text{FC}^T(\mathbf{u}_1, \dots, \mathbf{u}_K, P; \Theta_{\text{aux}}^T)), \end{aligned} \quad (28)$$

where the output vectors of the receiver DNNs before binarization, i.e., $\mathbf{u}_k = \text{FC}_k^R(\mathbf{h}_k^{\text{Re}}, \Theta_k^R)$, $k = 1 \dots, K$, are taken as the input values of the auxiliary transmitter DNN. This is the primary difference between the auxiliary DNN and the existing transmitter DNN described in (18) (the parameter set Θ_{aux}^T for training is also different).

Based on (28), the entire network obtained after removing both the binarization and hyperbolic tangent layers from each receiver DNN and then concatenating the remaining receiver DNNs with the auxiliary transmitter DNN can be considered as a single fully connected network (the overall network connected with blue dashed lines in Fig. 1); thus, there is no quantization error in the training of this network. Note that the conventional transmitter DNN accepts binary values as input values, whereas the auxiliary transmitter DNN accepts real

Algorithm 1 Joint training with auxiliary DNN

```

1: Initialize  $\Theta_k^R, \Theta_{aux}^T, \Theta^T$ ;
2: for  $l = 1 : num\_iterations$  do
3:   Generate channel data of each users as much as mini-
     batch  $\mathcal{B}$ ;
4:   Update  $FC_k^R(\Theta_k^R)$  and  $f^T(\Theta_{aux}^T)$  by minimizing
      $L_{aux}$ ;
5:   Update  $f_k^R(\Theta_k^R)$  and  $f^T(\Theta^T)$  by minimizing  $L_{main}$ ;
6: end for

```

Algorithm 2 Two-stage training with auxiliary DNN

```

1: # Pre-training stage
2: Initialize  $\Theta_k^R, \Theta_{aux}^T$ ;
3: for  $l = 1 : num\_iterations$  do
4:   Generate channel data of each users as much as mini-
     batch  $\mathcal{B}$ ;
5:   Update  $FC_k^R(\Theta_k^R)$  and  $f^T(\Theta_{aux}^T)$  by minimizing
      $L_{aux}$ ;
6: end for
7:
8: # Fine-tuning stage
9: Initialize  $\Theta^T$  based on pre-trained  $\Theta_{aux}^T$ ;
10: Initialize  $\Theta_k^R$  based on pre-trained  $\Theta_k^R$ ;
11: for  $l = 1 : num\_iterations$  do
12:   Generate channel data of each users as much as mini-
     batch  $\mathcal{B}$ ;
13:   Update  $f_k^R(\Theta_k^R)$  and  $f^T(\Theta^T)$  by minimizing  $L_{main}$ ;
14: end for

```

values as input values. Similar to (25)-(26), the optimization problem with the auxiliary network is defined as

$$\min_{\Theta_{aux}^T, \Theta_1^R, \dots, \Theta_K^R} L_{aux}(\{\Theta_k^R\}_{k=1}^K, \Theta_{aux}^T), \quad (29)$$

where

$$\begin{aligned} L_{aux}(\{\Theta_k^R\}_{k=1}^K, \Theta_{aux}^T) \\ = - \sum_{k=1}^K R_k(f^T(\{FC_k^R(\mathbf{h}_k^{\text{Re}}; \Theta_k^R)\}_{k=1}^K, P; \Theta_{aux}^T)). \end{aligned} \quad (30)$$

To utilize the auxiliary transmitter DNN in the training phase, we employ a joint training method that alternatively trains the shallow student network (existing transmitter DNN) and the deep teacher network (auxiliary transmitter DNN) [23], [24]. The detailed procedure of joint training is described in Algorithm 1. The auxiliary network and the main (existing) network are sequentially updated for each iteration. Consequently, the auxiliary transmitter DNN can guide the existing transmitter and receiver DNNs with useful information for generalization, and the corresponding joint training prevents the existing DNNs from being trapped at a poor local minimum when the network is trained from scratch [23], [24].

In contrast to joint training with a teacher network, we may consider another simple method for distilling knowledge, which uses a two-stage optimization. This method first optimizes the receiver DNN using an auxiliary transmitter

DNN, and then applies a hyperbolic tangent function and binarization operator to the outputs of the receiver DNNs. The network is fine-tuned with pre-trained parameters (Algorithm 2). However, for DNNs that include the quantization layer, such as the limited feedback system, joint training methods such as Algorithm 1 are more suitable than the two-stage training method. This is because, in the pre-training stage of Algorithm 2, the auxiliary transmitter DNN is trained without considering the effect of the quantization; thus, this model cannot produce an appropriate guidance signal for the existing transmitter and receiver DNNs in the fine-tuning stage [24]. In contrast, Algorithm 1 jointly trains the existing DNNs and the auxiliary DNN. The lossless gradient from the auxiliary DNN guides the generalization of the existing DNNs reflecting the quantization error from binarization. Thus, it achieve better performance. We empirically compare two training method in the following section.

IV. NUMERICAL RESULTS

A. Simulation setup

We use random matrix quantization (RMQ) for the baseline system, where randomly generated quantization codebooks are used for limited feedback. That is, codewords are independently and uniformly distributed in the set of all N -dimensional subspaces (or planes) passing through the origin in an M -dimensional space [6]. The total throughput of the system is evaluated using the sum rate, $\sum_{k=1}^K R_k$. For the baseline BD and RBD schemes, the expected signal-to-interference-plus-noise ratio (SINR) proposed in [12] is adopted as the distance measure of (2). This is because the expected SINR is an optimally designed distance measure for maximizing the multiplexing gain such that it generally achieves a higher sum rate than that achieved with the conventional chordal distance.

End-to-end supervised learning is performed with the following setup. Each receiver DNN consists of three-layer fully connected network with the dimensions $40MN$, $30MN$, $20MN$, and the transmitter DNN consists of three-layer fully connected network with the dimensions $20MNK$, $30MNK$, $40MNK$. The auxiliary transmitter DNN has the same structure (but different parameters Θ_{aux}^T) as the transmitter DNN. We set a batch size of 1000 with the Adam optimizer [36]. The training was conducted for 50000 iterations with an initial learning rate of 2×10^{-4} by reducing the rate by 0.1 times at the 30000th and 40000th iterations. For the experiment with $M = 8$, $N = 4$, the initial learning rate is set to 1×10^{-4} as an exception. For testing the learned DNNs, we evaluate 100,000 independently sampled test data. In addition, we use 100,000 independently sampled validation data to determine the best performing model. The algorithms were implemented using the TensorFlow 1.8.0 library.

The proposed deep-learning-based system is ideally designed by assuming that users have independent receiver DNNs. However, in realistic systems, performing end-to-end learning whenever a new user is attached to the BS is impractical (it requires too much computation time and bundle). Accordingly, we consider a special case assuming that the

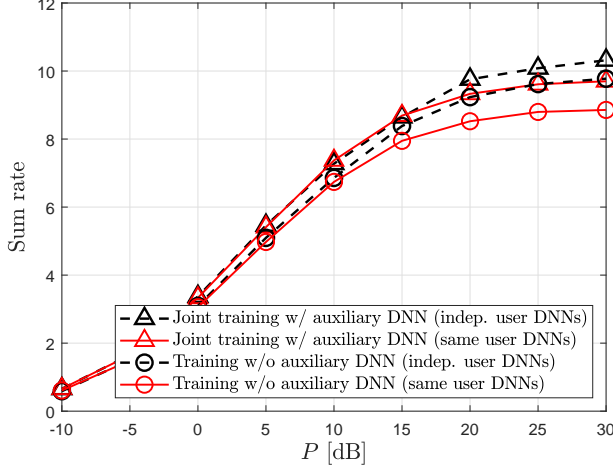


Fig. 2. Sum rate vs. P (dB). $M = 8$, $N = 2$, $K = 4$, and $B = 6$

users share the same receiver DNN (i.e., $f_1^R = f_2^R = \dots = f_K^R$ and $\Theta_1^R = \Theta_2^R = \dots = \Theta_K^R$) as a practical application. Then, a single receiver DNN trained offline can be used for any users associated to the BS. Although the performance will be enhanced if the users can have independent DNNs for training in an end-to-end manner, the difference between using the same user DNN and independent user DNNs will not be very large, unless the statistical distributions of the user channels are very different. Fig. 2 illustrates these observations; the performance with using different and independent DNNs for the users is better than when the same DNN is shared among the users, when P is high. However, the gain achieved using the auxiliary teacher network is larger when the users share the same DNN. This indicates that the proposed training with the auxiliary network can compensate for the performance degradation caused by forcing the users to share the same DNN in practical systems. Based on these observations, the simulation results in the following section are obtained assuming that the users share the same DNN, unless otherwise specified (because the corresponding results would be more useful for practical systems). Moreover, Algorithm 1 that employs an auxiliary teacher network for end-to-end training is applied, unless otherwise specified.

B. Simulation results

In this subsection, we first demonstrate the performance of zero-forcing precoding to emphasize the importance of the regularization parameter in limited feedback. In Fig. 3, the regularized methods generally and significantly outperform the normal zero-forcing precoding method. As discussed in Section II-C, with limited feedback, the regularization parameter α should be determined to reflect the effect of the quantization error. If we use the optimal value $\alpha = \frac{KN}{P}$ designed with perfect CSIT, the performances of RZF and RBD converge to those of normal ZF and BD, respectively, as the multiuser interference increases. For $N = 1$, an optimal regularization parameter was designed in [28], which is given by $\alpha = \frac{KN}{P}(1 + z^2)$, where z^2 includes the variance of the

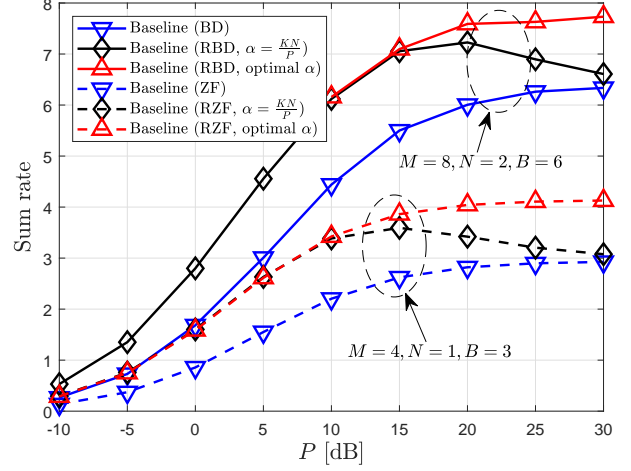


Fig. 3. Sum rate vs. $K = M/N$ and P (dB)

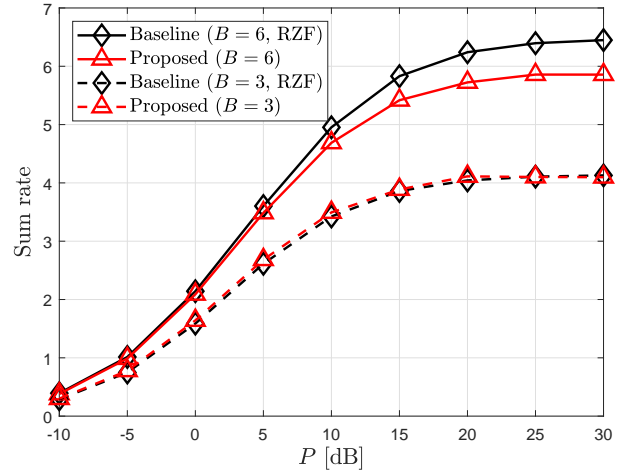


Fig. 4. Sum rate vs. P (dB). $M = 4$, $N = 1$, and $K = 4$

multiuser interference normalized by $\frac{KN}{P}$. However, if $N > 1$, the statistics of the multiuser interference are dependent on the distance measure used for quantization and are not known explicitly. Obtaining an explicit form of z^2 for $N > 1$ is difficult; thus, instead, we use the optimal value of z^2 numerically obtained based on an exhaustive search in the range between 0 and the maximum value of the multiuser interference divided by $\frac{KN}{P}$. Unless otherwise specified, the numerically determined optimal values of the regularization parameter (which are different for different M , N , B , and P) are used for the RBD in this section. It should be noted that the proposed scheme can outperform such a numerically optimized (thus infeasible in practical systems) RBD.

In Fig. 4, the sum rate achieved by the proposed deep-learning-based scheme is compared with those of the baseline schemes for two cases $B = 3$ and $B = 6$, when each user has a single receive antenna and $M = 4$. The proposed scheme shows a similar performance as the baseline RZF when $B = 3$ and exhibits lower performance when $B = 6$.

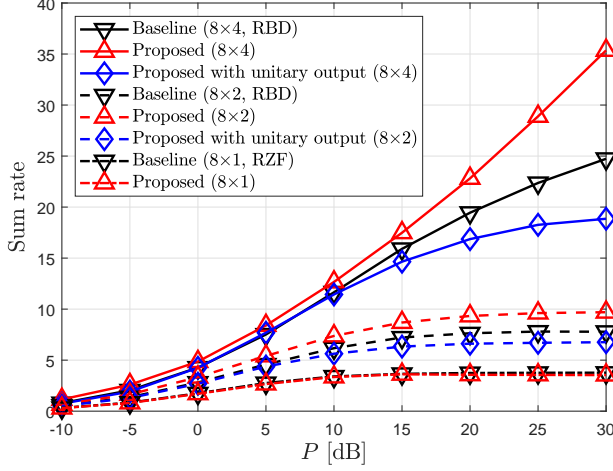


Fig. 5. Sum rate vs. P (dB). The total number of feedback bits is fixed, i.e., $BK = 24$ where $K = M/N$

The corresponding results show that the proposed DNN-based quantization and beamforming selection may not be useful when $N = 1$. Some gain can be obtained from joint channel estimation and quantization as demonstrated in a previous study [21]; however, the gain would not be significant.

In contrast, Fig. 5 shows that the proposed scheme can significantly outperform the baseline scheme when $N > 1$. The sum rate is compared by increasing the number of receive antennas while M is fixed to 8. If $N = 1$, similar to the case in Fig. 4, the proposed scheme shows a performance similar to that of the baseline scheme. However, when $N > 1$, the proposed scheme achieves a much higher sum rate than the baseline scheme and the gain increases with N at a high P . The relatively poor performance of RBD is due to the difficulties in optimizing the limited feedback system when $N > 1$. That is, if $N > 1$, the CDI is given by a unitary matrix, and thus, codewords for quantization (in \mathcal{C}_k) are generally given by unitary matrices. However, it is very difficult to determine a distance measure between two unitary matrices that optimally decreases multiuser interference; this is also related to the difficulty in obtaining an optimal quantization codebook. Moreover, the columns of each precoding matrix of the conventional RBD are given by orthogonal vectors because this is a good choice with perfect CSIT. However, in limited feedback, an optimal precoding matrix may not have orthogonal columns. In fact, our deep-learning-based solution for precoding matrices does not have orthogonal columns, which indirectly shows the inefficiency of selecting orthogonal vectors with limited feedback.

For a further discussion, a modified version of the proposed deep-learning-based method, in which the precoding matrix of each user produced by the transmitter DNN is restricted to a unitary matrix, is also considered; the corresponding results are labeled as “proposed with unitary output” in Fig. 5. The output of the transmitter DNN can be restricted to a unitary matrix by applying Gram-Schmidt orthogonalization at each iteration of the end-to-end learning. The RBD achieves higher sum rates

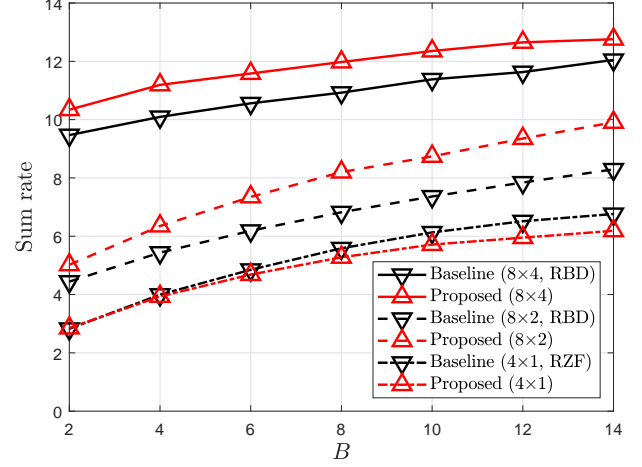


Fig. 6. Sum rate vs. B (dB). $K = M/N$ and $P = 10$ dB

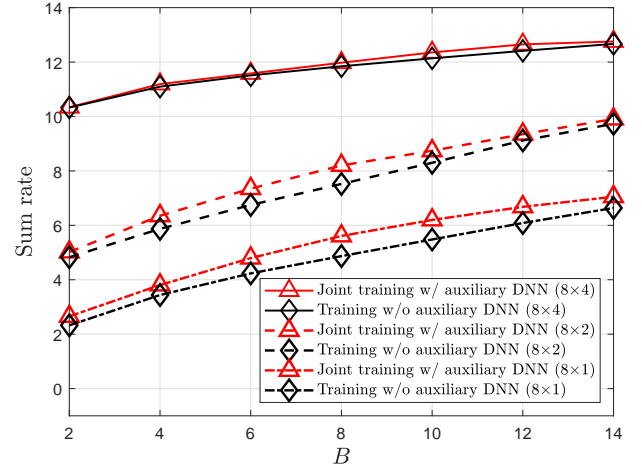


Fig. 7. Sum rate vs. B (dB). $K = M/N$ and $P = 10$ dB

than that of the proposed scheme with unitary output. That is, the RBD efficiently determines a good solution inside the set of matrices with orthogonal columns; however, a better solution exists outside the set with limited feedback. In Fig. 6, the sum rate is compared with respect to the number of feedback bits. When $N = 1$, similar to the case in Fig. 4, the proposed scheme achieves lower sum rates than those of the baseline scheme, and the sum rate gap increases with the number of feedback bits. When $N > 1$, the proposed scheme generally outperforms the baseline as expected in Fig. 5.

The use of an auxiliary (teacher) DNN to enhance the accuracy of end-to-end learning is a primary subject in this study. Figs. 7 and 8 show the performance enhancement achieved by introducing the auxiliary DNN, which can be used to mitigate gradient mismatches induced by adopting the binarization layer with STE to emulate the quantization process, as described in Section III. The sum rates of the proposed joint training with the auxiliary DNN are generally higher than those of the training without the auxiliary DNN.

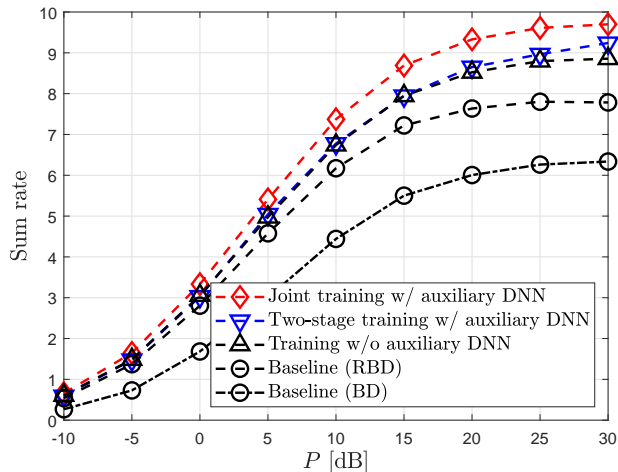


Fig. 8. Sum rate vs. P (dB). $M = 8$, $N = 2$, $K = 4$, and $B = 6$

The proposed training is useful at a moderate B for a fixed P as well as at a moderate and high P for a fixed B . Multiuser interference is relatively dominant for these cases, which indicates that the proposed joint training with the auxiliary DNN is particularly suitable when the number of feedback bits is insufficient. Moreover, the advantage of using an auxiliary DNN is enhanced as the number of users increases. As shown in Fig. 8, two-stage training with the auxiliary DNN achieves marginal gain compared with training without the auxiliary DNN. This implies that for training systems using quantization, such as limited feedback, using a pre-trained network without considering the quantization process for two-stage training may not be suitable for mitigating the performance loss caused by quantization error [24]. In contrast, joint training with auxiliary DNN achieves significant gain at a moderate and high P . This is because the auxiliary DNN can guide, at every iteration, the generalization of existing DNNs while considering the quantization error. In conclusion, joint training prevents the existing DNNs from being trapped at a poor local minimum in the training phase. At high SNR, the sum-rate difference between the proposed deep-learning-based scheme and the baseline RBD scheme is approximately two times greater with the auxiliary DNN than the difference without the auxiliary DNN.

In the proposed scheme, the output of the transmitter DNN varies with the transmit power, as the loss function is given by the downlink sum rate including the transmit power (3). If we attempt to train DNNs for each transmit power, we may require infinite DNNs, as the transmit power P is a continuous real variable; this is not feasible in practical systems. Thus, in this study, we also consider a unified transmitter DNN that can appropriately construct precoding matrices for any value of P in a fixed range. In particular, we additionally consider a method that trains our DNNs by considering the dB scale value of P as a uniform random variable in a certain range, independent of the channel. In this section, the range of P dB is set to $[-10, 30]$ dB. Fig. 9 shows the effectiveness of the corresponding method. If we use fixed DNNs trained with

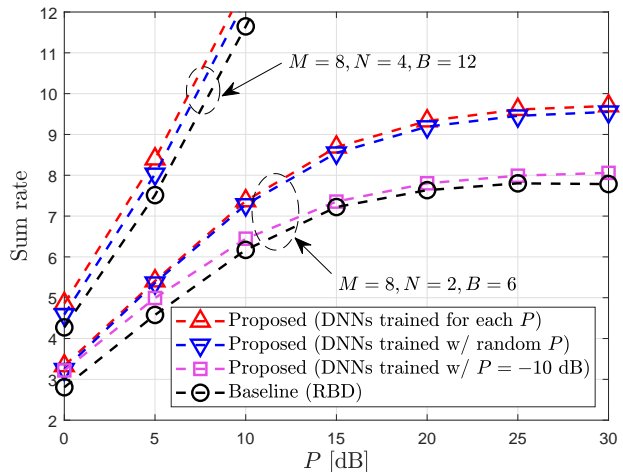


Fig. 9. Sum rate vs. P (dB). $K = M/N$

a fixed value of P to construct the precoding matrices for downlink transmission at different values of P (dashed line with square marker), the proposed scheme may not achieve the performance expected based on using individually trained DNNs for each P (dashed line with a regular triangle marker, optimal case). In contrast, if we train the DNNs by taking P as a random variable in $[-10, 30]$ dB, as discussed above (dashed line with reverse triangle marker), the performance of the proposed scheme is similar to that of the optimal case.

V. CONCLUSIONS

In this study, a deep-learning-based channel quantization, feedback, and precoding selection scheme was proposed for MU-MIMO systems. The role of the conventional codebook-based channel quantization process is replaced by a receiver DNN for each user, and the precoding selection is replaced by a transmitter DNN. A binarization layer was adopted to enable end-to-end learning, and the performance degradation caused by the binarization layer was effectively mitigated by an auxiliary (teacher) transmitter DNN used only in the training phase. The auxiliary transmitter DNN is connected to the receiver DNNs before quantization. Accordingly, by providing lossless gradients directly, it can prevent the receiver DNNs from being trapped at a poor local minimum. The proposed deep-learning-based system jointly trained with the teacher network significantly outperformed the conventional normal and regularized zero-forcing precoding when the number of receive antennas was greater than one, under the assumption of equal power allocation to the associated users. Appropriate solutions to a few practical issues regarding the difficulty of using different DNNs for users and the difficulty of training DNNs for every value of the transmitter power were also discussed.

In MU-MIMO downlink channels with limited feedback, the fairness or quality-of-service (QoS) of each user is an important issue as precoding does not achieve the expected performance with perfect CSIT due to the quantization error. In this study, we simply assumed equal power allocation

to consider a fair transmission; however, it still does not guarantee a minimum QoS for each user. Thus, a noteworthy direction for future research could be maximizing sum rate (possibly with power control) while satisfying a predefined QoS for each user. To achieve this, regularization terms that impose a QoS constraint can be added to the loss function (it was sum rate in this study) of end-to-end learning; however, in this case, the parameters for deep learning must be carefully optimized with reasonable expectation. Various approaches, including current studies in supervised-learning, can be used to achieve such an optimization.

REFERENCES

- [1] H. Weingarten, Y. Steinberg, and S. Shamai, "The capacity region of the Gaussian MIMO broadcast channel," in *Proc. IEEE ISIT*, Chicago, IL, June 2004.
- [2] G. Caire and S. Shamai, "On the achievable throughput of a multiantenna Gaussian broadcast channel," *IEEE Trans. Inf. Theory*, vol. 49, no. 7, pp. 1691–1706, July 2003.
- [3] N. Jindal and A. Goldsmith, "Dirty-paper coding versus TDMA for MIMO Broadcast channels," *IEEE Trans. Inf. Theory*, vol. 51, no. 5, pp. 1783–1794, May 2005.
- [4] L. U. Choi and R. D. Murch, "A transmit preprocessing technique for multiuser MIMO systems using a decomposition approach," *IEEE Trans. Wireless Commun.*, vol. 3, no. 1, pp. 20–24, Jan. 2004.
- [5] N. Jindal, "MIMO broadcast channels with finite-rate feedback," *IEEE Trans. Inform. Theory*, vol. 52, no. 11, pp. 5045–5060, Nov. 2006.
- [6] N. Ravindran and N. Jindal, "Limited feedback-based block diagonalization for the MIMO broadcast channel," *IEEE J. Sel. Areas Commun.*, vol. 26, no. 8, pp. 1473–1482, Oct. 2008.
- [7] D. J. Love, R. W. Heath Jr., and T. Strohmer, "Grassmannian beamforming for multiple-input multiple-output wireless systems," *IEEE Trans. Inf. Theory*, vol. 49, no. 10, pp. 2735–2747, Oct. 2003.
- [8] D. J. Love and R. W. Heath, Jr., "Limited feedback unitary precoding for spatial multiplexing systems," *IEEE J. Sel. Areas Commun.*, vol. 51, no. 8, pp. 2967–2976, Aug. 2005.
- [9] T. Yoo, N. Jindal, and A. Goldsmith, "Multi-antenna downlink channels with limited feedback and user selection," *IEEE J. Sel. Areas Commun.*, vol. 25, no. 7, pp. 1478–1491, Sep. 2007.
- [10] M. Trivellato, F. Boccardi, and H. Huang, "On transceiver design and channel quantization for downlink multiuser MIMO systems with limited feedback," *IEEE J. Sel. Areas Commun.*, vol. 26, no. 8, pp. 1494–1504, Oct. 2008.
- [11] D. Love et al., "An overview of limited feedback in wireless communication systems," *IEEE J. Sel. Areas Commun.*, vol. 26, no. 8, pp. 1341–1365, Oct. 2008.
- [12] M. Min, Y. S. Jeon, and G. H. Im, "On achievable multiplexing gain of BD in MIMO broadcast channels with limited feedback," *IEEE Trans. Wireless Commun.*, vol. 15, no. 2, pp. 871–885, Feb. 2016.
- [13] Q. H. Spencer, A. L. Swindlehurst, and M. Haardt, "Zero-forcing methods for downlink spatial multiplexing in multiuser MIMO channels," *IEEE Trans. Sig. Processing*, vol. 52, no. 2, pp. 461–471, Feb. 2004.
- [14] T. Yoo and A. Goldsmith, "On the optimality of multi-antenna broadcast scheduling using zero-forcing beamforming," *IEEE J. Sel. Areas Commun.*, vol. 24, no. 3, pp. 528–541, Mar. 2006.
- [15] C. Peel, B. Hochwald and A. Swindlehurst, "Vector-perturbation technique for near-capacity multi-antenna multiuser communication-Part I: Channel inversion and regularization," *IEEE Trans. Commun.*, vol. 53, no. 1, pp. 195–202, Jan. 2005.
- [16] V. Stankovic and M. Haardt, "Generalized design of multiuser MIMO precoding matrices," *IEEE Trans. Wireless Commun.*, vol. 7, pp. 953–961, Mar. 2008.
- [17] C.-K. Wen, W.-T. Shih, and S. Jin, "Deep learning for massive MIMO CSI feedback," *IEEE Wireless Commun. Lett.*, vol. 7, no. 5, pp. 748–751, Oct. 2018.
- [18] T. Wang, C.-K. Wen, S. Jin, and G. Y. Li, "Deep learning-based CSI feedback approach for time-varying massive MIMO channels," *IEEE Wireless Commun. Lett.*, vol. 8, no. 2, pp. 416–419, Apr. 2019.
- [19] C. Lu, W. Xu, H. Shen, J. Zhu, and K. Wang, "MIMO channel information feedback using deep recurrent network," *IEEE Commun. Lett.*, vol. 23, no. 1, pp. 188–191, Jan. 2019.
- [20] Y. Jang, G. Kong, M. Jung, S. Choi, and I.-M. Kim, "Deep autoencoder based CSI feedback with feedback errors and feedback delay in FDD massive MIMO systems," *IEEE Wireless Commun. Lett.*, vol. 8, no. 3, pp. 833–836, Jun. 2019.
- [21] J. Jang, H. Lee, S. Hwang, H. Ren, and I. Lee, "Deep learning-based limited feedback designs for MIMO systems," *IEEE Wireless Commun. Lett.*, vol. 9, no. 4, pp. 558–561, Apr. 2020.
- [22] Bengio, Yoshua and Léonard, Nicholas and Courville, Aaron, "Estimating or propagating gradients through stochastic neurons for conditional computation," *arXiv preprint arXiv:1308.3432* 2013.
- [23] Zhuang, Bohan and Shen, Chunhua and Tan, Mingkui and Liu, Lingqiao and Reid, Ian, "Towards effective low-bitwidth convolutional neural networks," in *Proc. IEEE conference on computer vision and pattern recognition*, pp. 7920–7928, 2018.
- [24] Zhuang, Bohan and Liu, Jing and Tan, Mingkui and Liu, Lingqiao and Reid, Ian and Shen, Chunhua, "Effective training of convolutional neural networks with low-bitwidth weights and activations," *arXiv preprint arXiv:1908.04680* 2019.
- [25] F. Sohrabi, K. M. Attiah, and W. Yu, "Deep Learning for Distributed Channel Feedback and Multiuser Precoding in FDD Massive MIMO," *arXiv preprint arXiv:2007.06512* 2020.
- [26] S. Christensen, R. Agarwal and J. M. Cioffi, "Weighted sum-rate maximization using weighted MMSE for MIMO-BC beamforming design," *IEEE Trans. Wireless Commun.*, vol. 7, no. 12, pp. 4792–4799, Dec. 2008.
- [27] R. Fritzsche and G. P. Fettweis, "Robust sum rate maximization in the multi-cell MU-MIMO downlink," *Proc. IEEE WCNC*, pp. 3180–3184, Apr. 2013.
- [28] Z. Wang and W. Chen, "Regularized zero-forcing for multi-antenna broadcast channels with user selection," *IEEE Wireless Commun. Lett.*, vol. 1, no. 2, pp. 129–132, Apr. 2012.
- [29] LeCun, Yann and Bengio, Yoshua and Hinton, Geoffrey, "Deep learning," *nature*, vol. 521, no. 7553, pp. 436–444, 2015.
- [30] Zhuang, Bohan and Liu, Lingqiao and Tan, Mingkui and Shen, Chunhua and Reid, Ian, "Training Quantized Neural Networks with a Full-precision Auxiliary Module," in *Proc. IEEE conference on computer vision and pattern recognition*, pp. 1488–1497, 2020.
- [31] Hinton, Geoffrey and Vinyals, Oriol and Dean, Jeff, "Distilling the knowledge in a neural network," in *Proc. Adv. Neural Inf. Process. Syst. Workshops, (NIPSW)*, 2014.
- [32] Ba, Jimmy and Caruana, Rich, "Do deep nets really need to be deep?," in *Proc. Adv. Neural Inf. Process. Syst. (NIPS)*, pp. 2654–2662, 2014.
- [33] Romero, Adriana and Ballas, Nicolas and Kahou, Samira Ebrahimi and Chassang, Antoine and Gatta, Carlo and Bengio, Yoshua, "Fitnets: Hints for thin deep nets," in *Proc. Int. Conf. Learn. Represent. (ICLR)*, 2015.
- [34] Parisotto, Emilio and Ba, Jimmy Lei and Salakhutdinov, Ruslan, "Actor-mimic: Deep multitask and transfer reinforcement learning," in *Proc. Int. Conf. Learn. Represent. (ICLR)*, 2016.
- [35] Zadoruyko, Sergey and Komodakis, Nikos, "Paying more attention to attention: Improving the performance of convolutional neural networks via attention transfer," in *Proc. Int. Conf. Learn. Represent. (ICLR)*, 2017.
- [36] Kingma, Diederik P and Ba, Jimmy, "Adam: A method for stochastic optimization," *arXiv preprint arXiv:1412.6980* 2014.